

Experimental Test of the Axion Paradigm using Quantum Sensing

Phase-Resolved Haloscope with Magnetic Tunability

Jeanne BALLY

PhD student in HQC's group, LPENS - LPEM

Exp : C. Fruy, K. Kodama, D. Diez, A. Théry, B. Hue, T. Fauvet, L. Jarjat, T. Philippe Kagan, M.R. Delbecq, T. Kontos

Theory : A. Cottet

RADES Collaboration : I. Irastorza, S. Paraonau, W. Wernsdorfer (Dark Quantum) + B. Döbrich, A. Lindner...

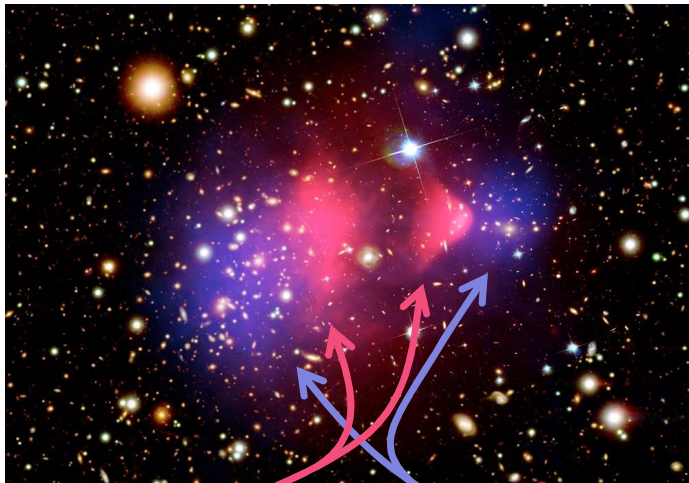


The Dark Universe

Dark matter: hypothetical matter that interacts weakly ordinary matter.

The bullet cluster (ESA)

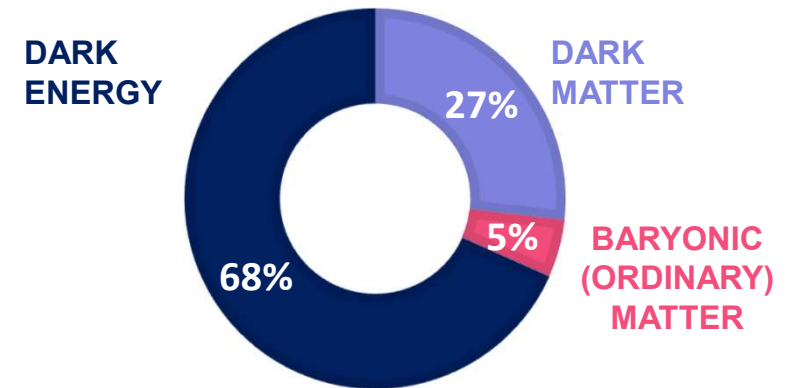
X-ray:
NASA/CXC/Cf
A/M.Markevitch
Optical and
lensing map:
NASA/STScI,
Magellan/U.Arizona/D.Clowe
Lensing map:
ESO WFI



Hot intracluster gas detected in **X-ray** (contains most of the baryonic matter)

Gravitational lensing detected mass

Estimated matter-energy content of the Universe :



➔ Non-zero local dark matter density, with extremely weak interactions with standard matter

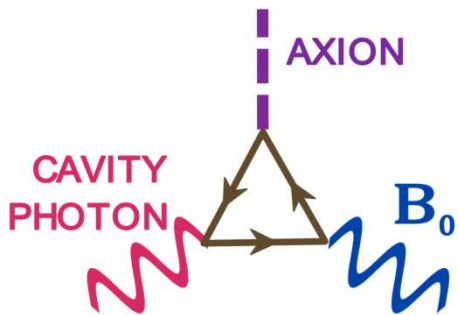
The **AXION** particle
➔ good Dark Matter candidate

The Axion Particle

- Solve the strong charge-parity (CP) problem
- Peccei-Quinn solution: spontaneous breaking of symmetry

R.D. Peccei and H.R. Quinn, PRL'77, Weinberg, PRL'78, Wilczek, PRL'78...

Primakoff effect

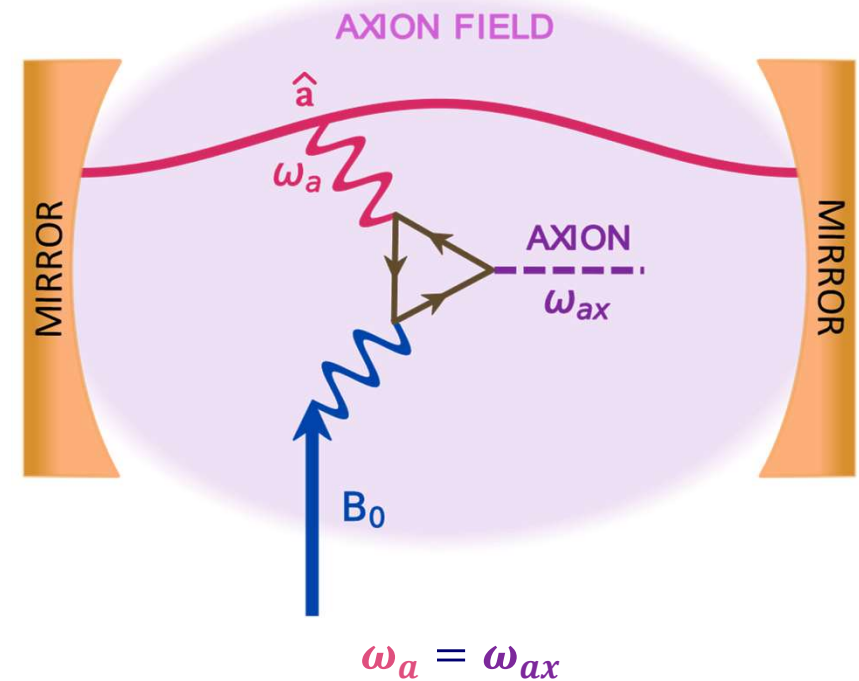


Lagrangian axion–photon interaction term:

$$g_{\alpha\gamma\gamma} \Phi_{ax} \cos(\omega_{ax} t) \vec{E} \cdot \vec{B}_0$$

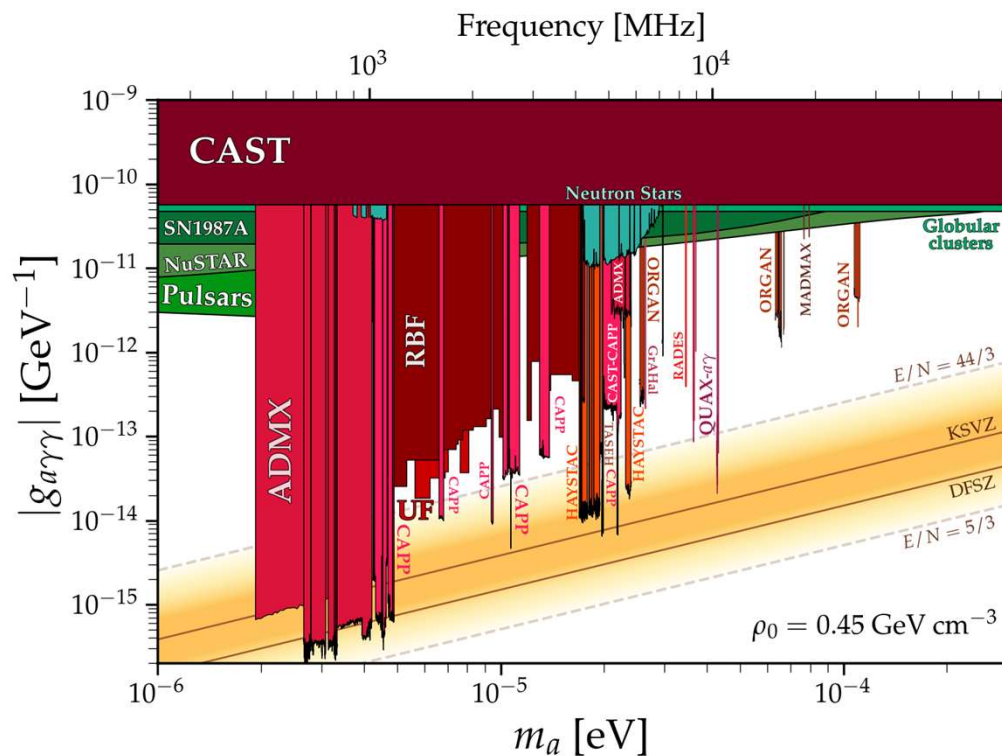
P. Sikivie, PRL 51, 1415 (1983)

Laboratory searches via electromagnetic conversion experiments: **HALOSCOPES**



The Axion Search

Parameter space explored by axion experiments benchmarked by **KSVZ** and **DFSZ** predicted axion mass and coupling strength



$g_{a\gamma\gamma}$: coupling constant
 m_a : axion mass

Challenges in axion searches:

- Weak signal $\sim 10^{-24}$ to 10^{-22} W
- Narrow linewidth ~ 1 kHz
- Unknown mass $m_a \sim$ microwave range ($\omega_{ax} \sim 0.1$ GHz to 0.1 THz)

Previous experiments have a **low tunability** with \sim MHz detection bands at fixed cavity frequency

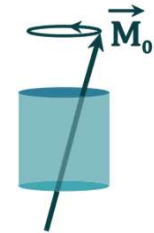
Research Project Goals

Key goals of AXION sensing:

➤ Expand the **mass scanning range**



Magnetic materials in resonant cavities



➤ Boost the **detection sensitivity**



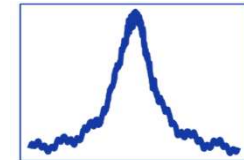
Non-linear coupling



➤ Simulate a **fake axion** signal



Phase-jammed signal



Research Project Goals

Key goals of AXION sensing:

➤ Expand the **mass scanning range**



Magnetic materials in resonant cavities



➤ Boost the **detection sensitivity**



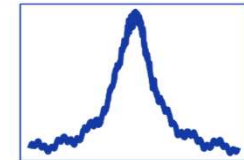
Non-linear coupling



➤ Simulate a **fake axion** signal

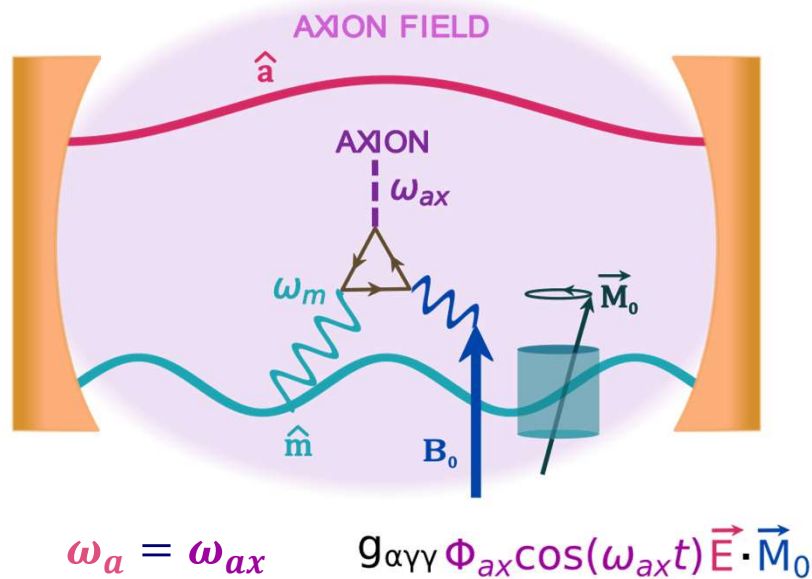


Phase-jammed signal



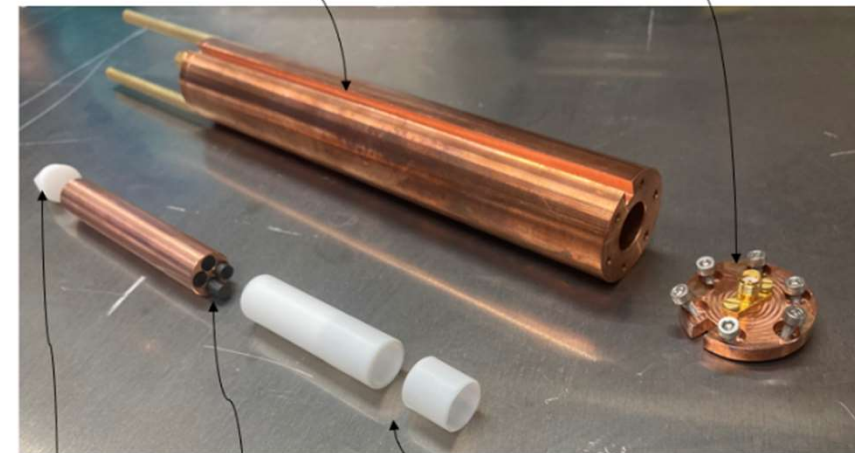
Magnetic Tunability

Ferromagnetic cavity



Copper cavity

Cavity's hat



Teflon support YIG rods Teflon support

YIG crystals permeability tensor : frequency and magnetic resonance dependence

$$\check{\mu}(\omega) = \mu_0 \begin{bmatrix} \mu_r(\omega) & i\mu_a(\omega) & 0 \\ -i\mu_a(\omega) & \mu_r(\omega) & 0 \\ 0 & 0 & 1 \end{bmatrix} \xrightarrow[\text{Gilbert equation}]{\text{Landau-Lisnitz-}} \mu_r = \frac{\omega_H(\omega_M + \omega_H) - \omega^2}{\omega_H^2 - \omega^2}, \quad \mu_a = \frac{\omega\omega_M}{\omega_H^2 - \omega^2}$$

$$\omega_M = \mu_0\gamma M_0, \quad \omega_H = \mu_0\gamma H_0 + i\eta\omega$$

Gyromagnetic Modes

$$\check{\mu}(\omega) = \mu_0 \begin{bmatrix} \mu_r(\omega) & i\mu_a(\omega) & 0 \\ -i\mu_a(\omega) & \mu_r(\omega) & 0 \\ 0 & 0 & 1 \end{bmatrix}$$

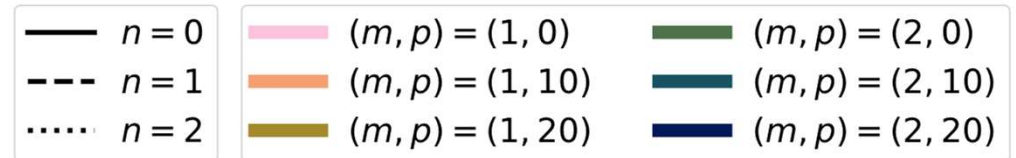
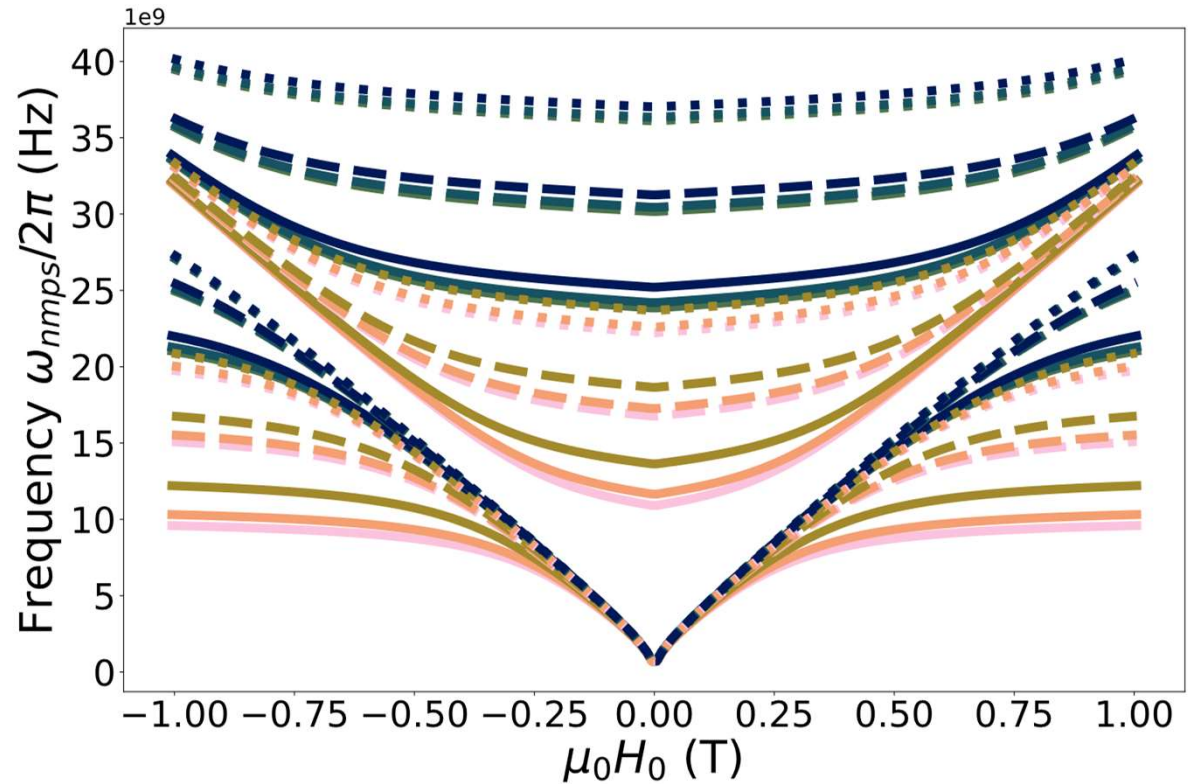
Maxwell equations
in a cylindrical
cavity



$$\omega_{nmp} = \frac{k_{nmp}}{\sqrt{\mu_{\perp}}\epsilon} = \sqrt{\left(\frac{z_{nm}}{a}\right)^2 + \left(\frac{p\pi}{L}\right)^2} \frac{1}{\sqrt{\mu_{\perp}}\epsilon}$$

with $\mu_{\perp} = \mu_0 \frac{\mu_r^2 - \mu_a^2}{\mu_r}$

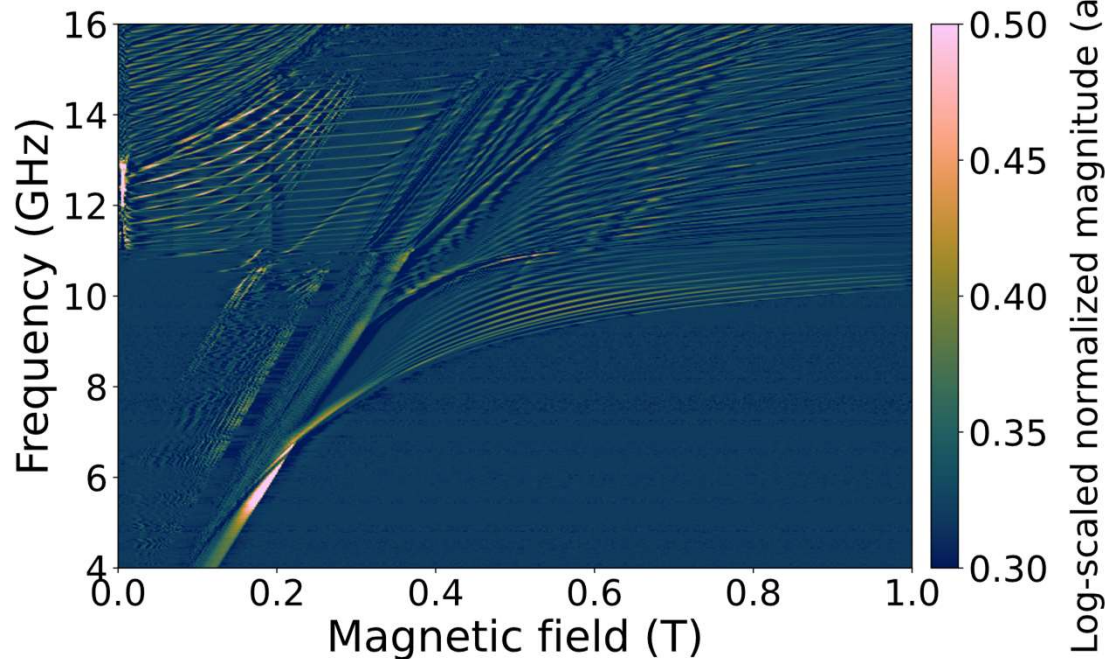
(n, m, p) = angular, radial and longitudinal modes



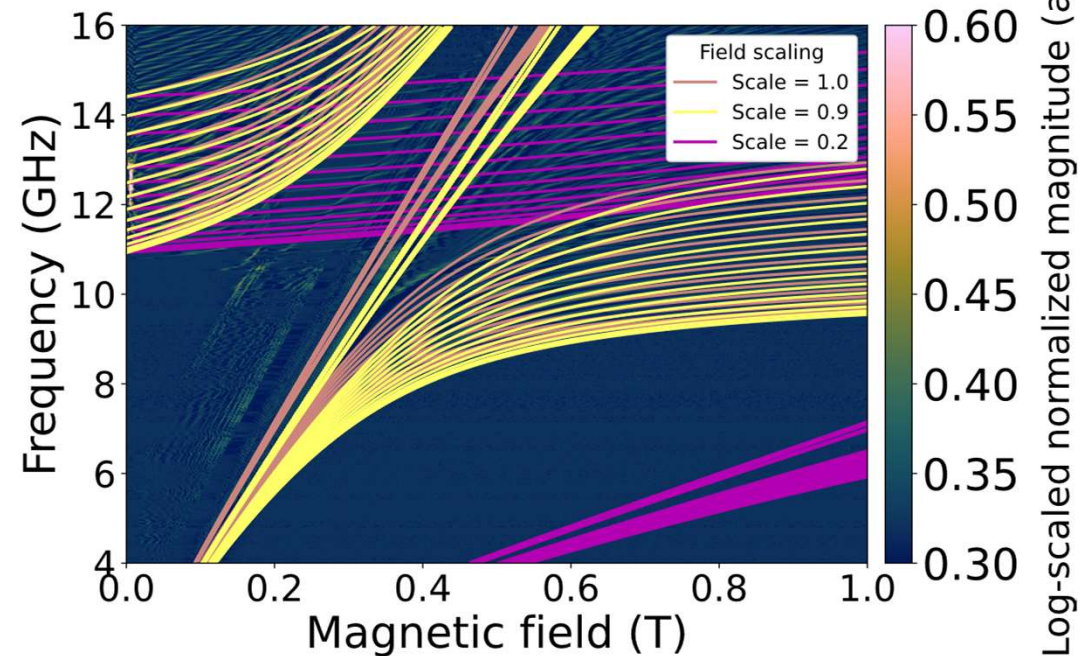
$\omega_{0,1,0,\pm 1}$ slope = 28 GHz/T

Experimental Results

YIG magnetospectroscopy 20mK



Inhomogeneous B field model overlay



Achieved **28.4 GHz/T slope**, in addition to good understanding of the dispersion with **analytical** approach

High spectral density of gyromagnetic modes, including modes with lower slope than expected

On-going **analysis** to identify additional, Comsol **simulation**

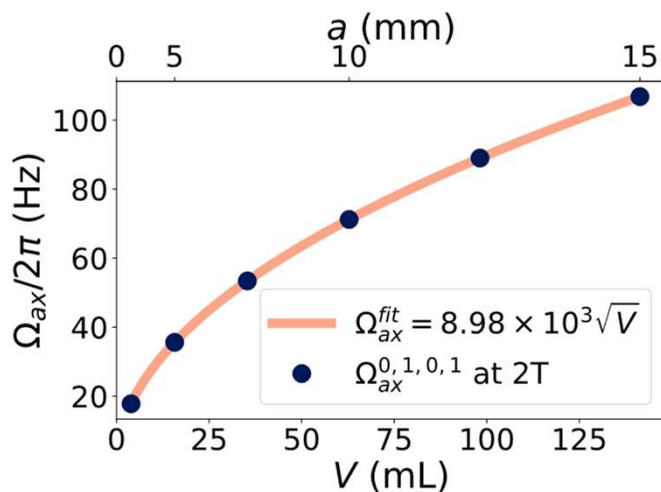
Axion-Photon Coupling

$$\Omega_{ax}^m = \frac{1}{\hbar\mu_0 c} g_{a\gamma\gamma} \mu_0 (M_0 + H_0) \frac{1}{z_{0m}} \sqrt{\frac{2V}{\epsilon}} \hbar\omega_{0m}$$

➤ $\frac{1}{m}$ scaling

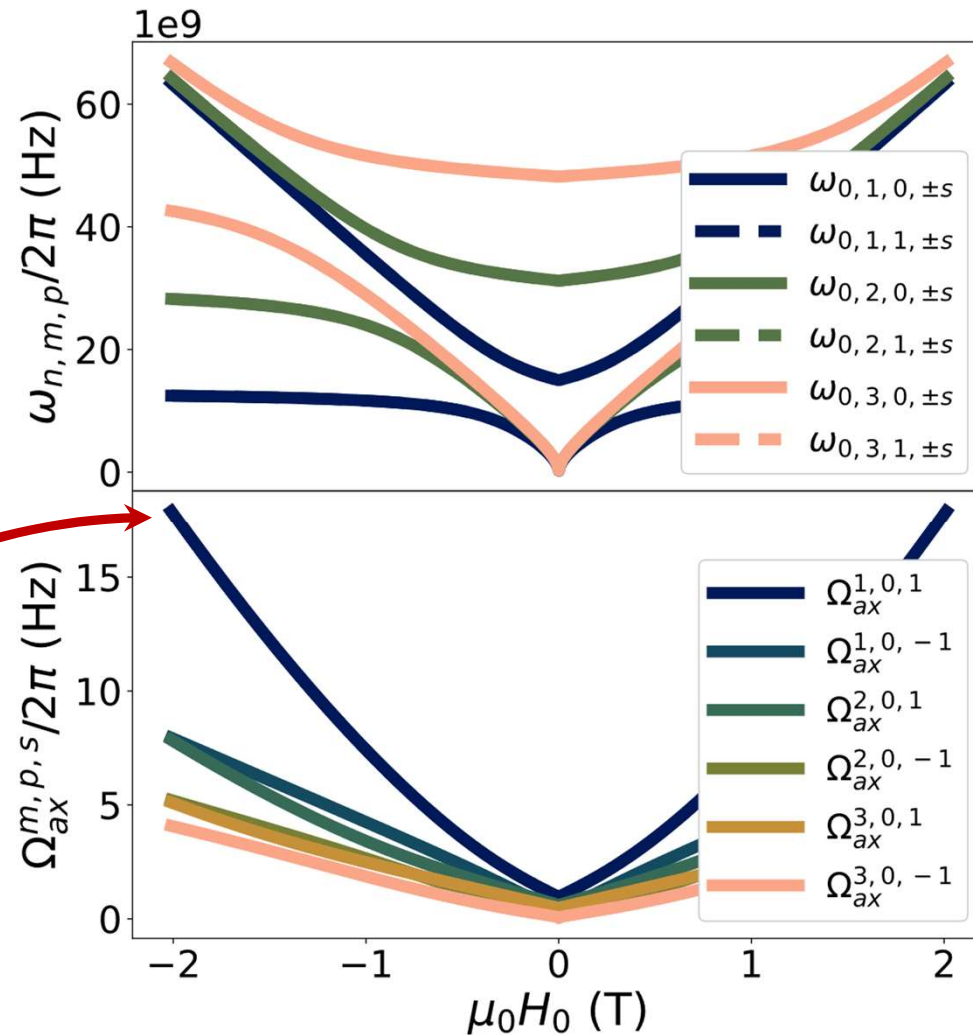
➔ focus on $(n, m, p) = (0, 1, 0) \equiv TM_{010}$ mode

➤ \sqrt{V} scaling → a higher axion field volume leads to a stronger coupling



18 Hz coupling strength for **1 cavity** of radius $a = 2.5$ mm $\equiv V \approx 3.9$ mL

Cavity paralleling?
 $V_{eff} = NV_{cav}$



Conventional Haloscope FoM

Figure of Merit (FoM): $F = \frac{1}{T}$ with T the minimum time to get $SNR = 1$

FoM for tunable haloscope: $F_{halo}^m = \frac{(\Omega_{ax}^0)^4}{\Lambda_a^3}$

$$\Omega_{ax}^0 = g_{\alpha\gamma\gamma} \frac{\mu_0(M_0 + H_0)}{\hbar\mu_0 c z_{0m}} \sqrt{\frac{2V}{\epsilon} \hbar\omega_{0m}}$$

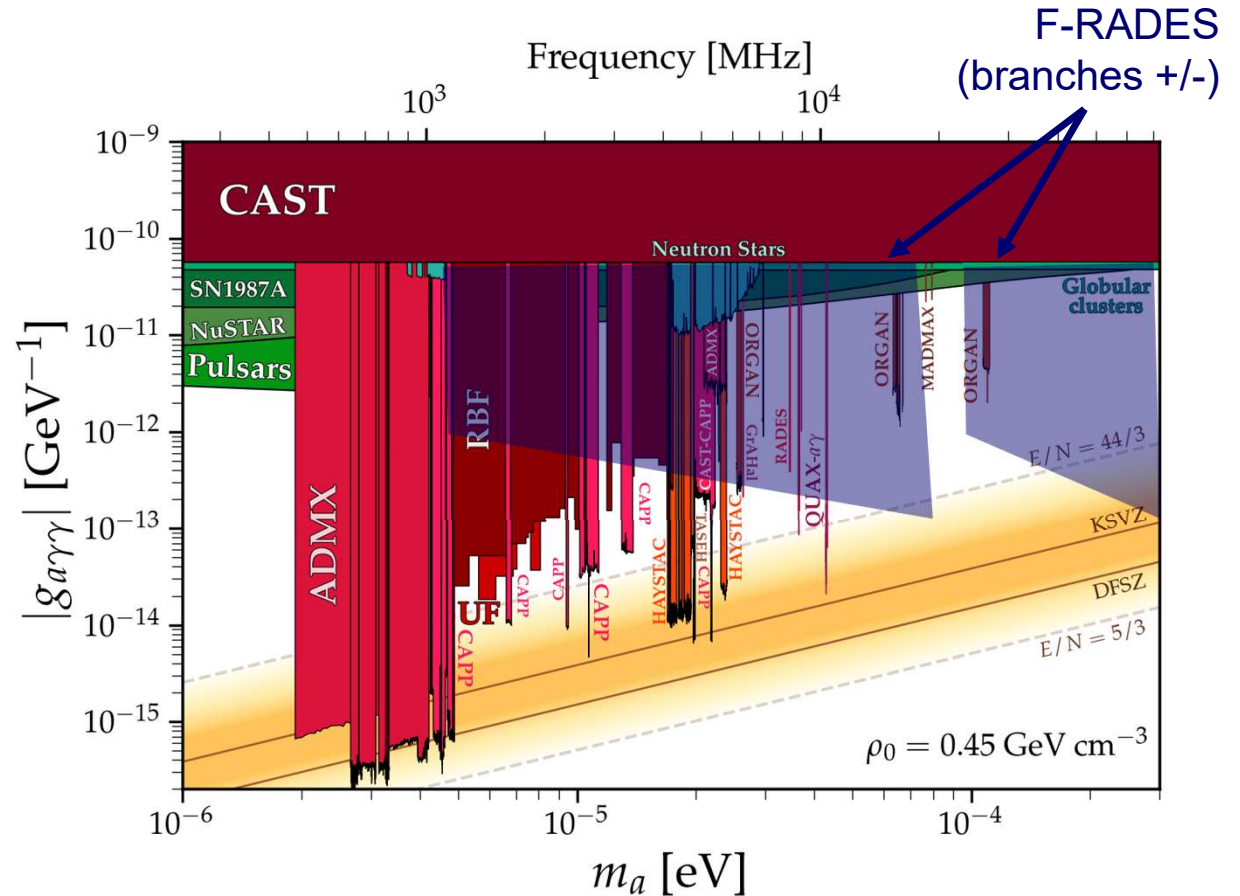
→ Coupling constant in GeV:

$$g_{\alpha\gamma\gamma}^{[eV^{-1}]} = g_{\alpha\gamma\gamma} \frac{m_a^{0m}}{\sqrt{2\rho_{ax}(\hbar c)^3}}$$

- RADES measurement time

$$F_{halo} = \frac{1}{T_{RADES}} = 10^{-5} \text{ Hz}$$

- Cavity quality factor $Q = 10^5$
- $SNR = 1$



→ 1.2 GHz to 66.8 GHz tunability

(Article in preparation)

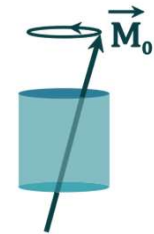
Research Project Goals

Key goals of AXION sensing:

➤ Expand the **mass scanning range**



Magnetic materials in resonant cavities



➤ Boost the **detection sensitivity**



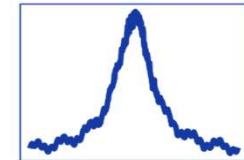
Non-linear coupling



➤ Simulate a **fake axion** signal



Phase-jammed signal



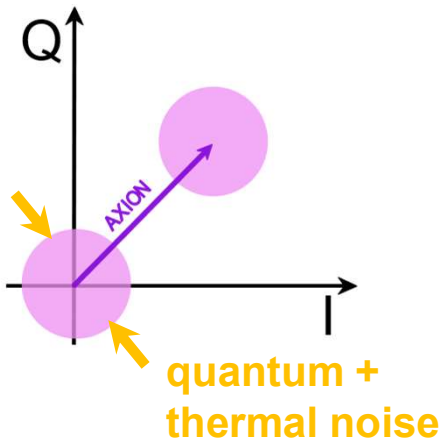
Quantum Detection Scheme

Phase-resolved haloscope with magnet tunability scheme

Conventional haloscope

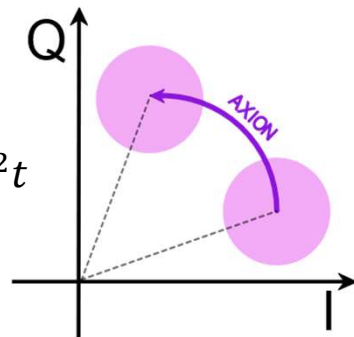
$$P \propto |\hat{a} + \hat{a}_{ax}|^2$$

with $\hat{a}_{ax} \ll \hat{a}$

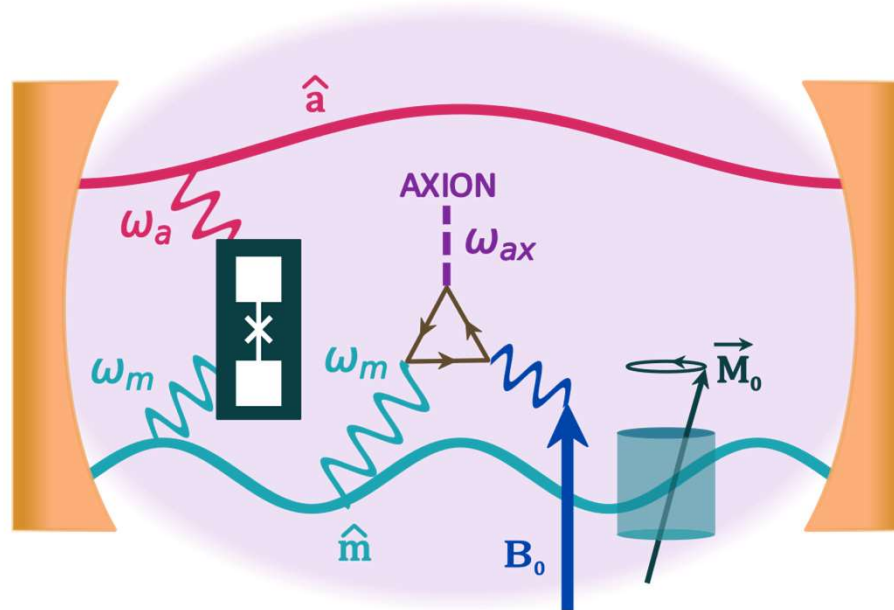


Non-linear coupling

$$\Delta\Phi \propto K|\hat{a} + \hat{a}_{ax}|^2 t$$



➔ Phase accumulation over time t



\hat{a} : cavity signal

\hat{a}_{ax} : axion signal

K : Kerr constant

t : interaction time

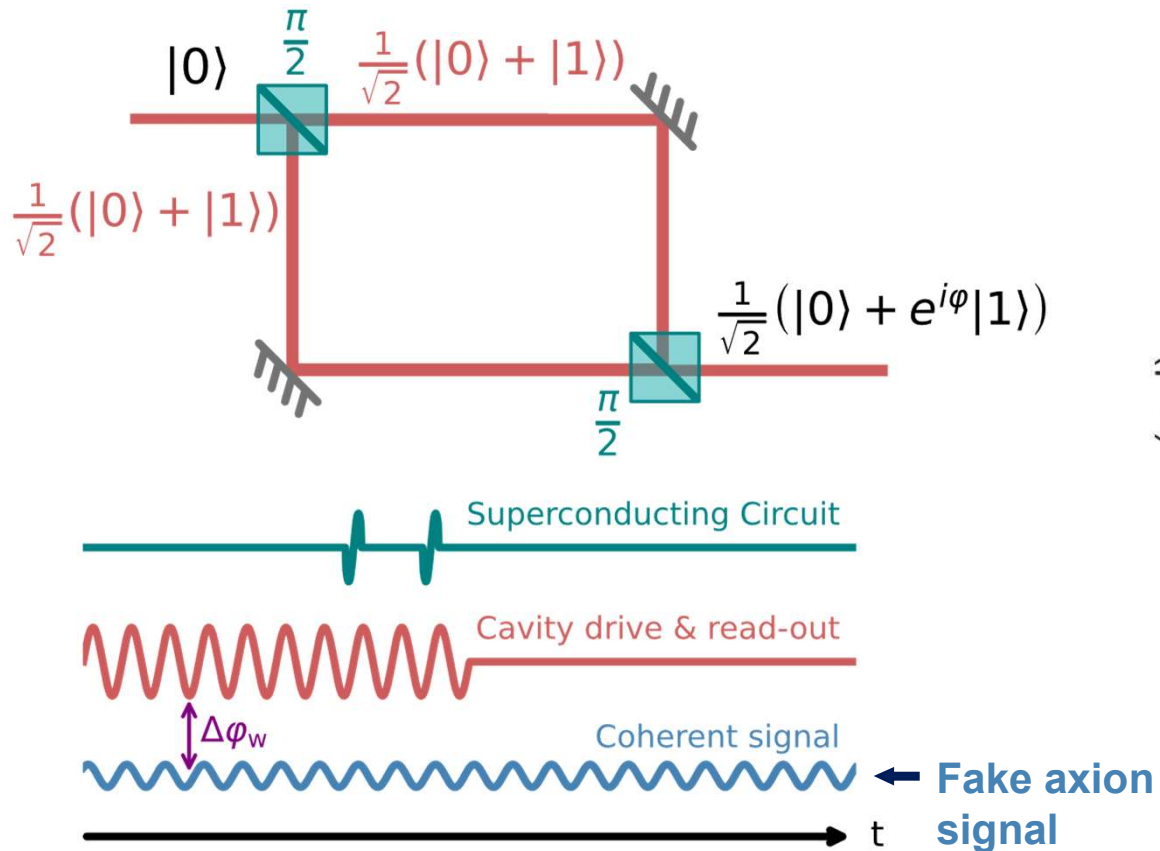
A. Cottet and T. Kontos: *New J Phys* 28 024504 (2026),
Gurevich and Melnikov (1996)

Cavity drive and axion field **interference term** from the superconducting circuit dispersively coupled

$$\Delta\omega_a \approx K [|\hat{a}|^2 + |\hat{a}_{ax}|^2 + 2|\hat{a}||\hat{a}_{ax}|\cos(\varphi_{ax})]$$

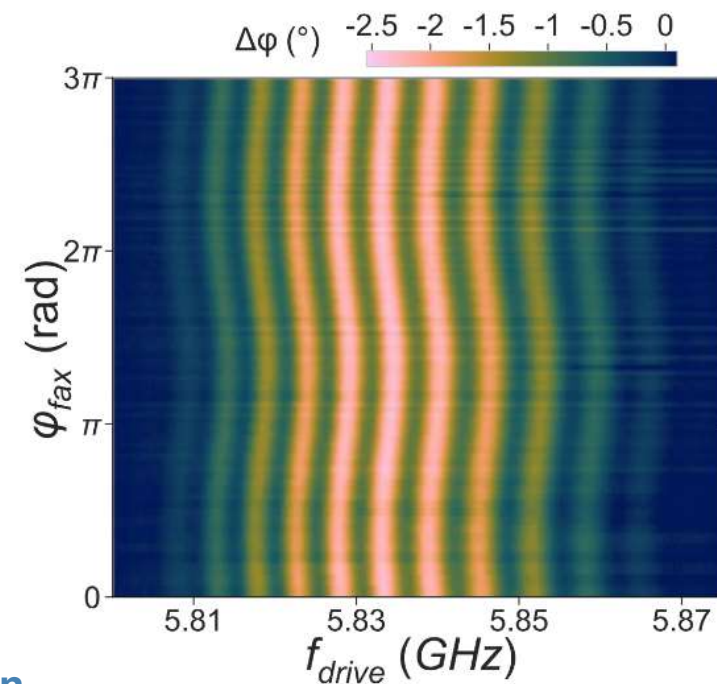
Non-Linear Quantum Interferometry

Ramsey experiment on fake-axion signal



$$\Delta\phi_\omega \sim -\frac{2K g^2}{\kappa \Delta^2} |\sqrt{n_{cav}} + \sqrt{n_\omega} e^{i\phi_\omega}|^2$$

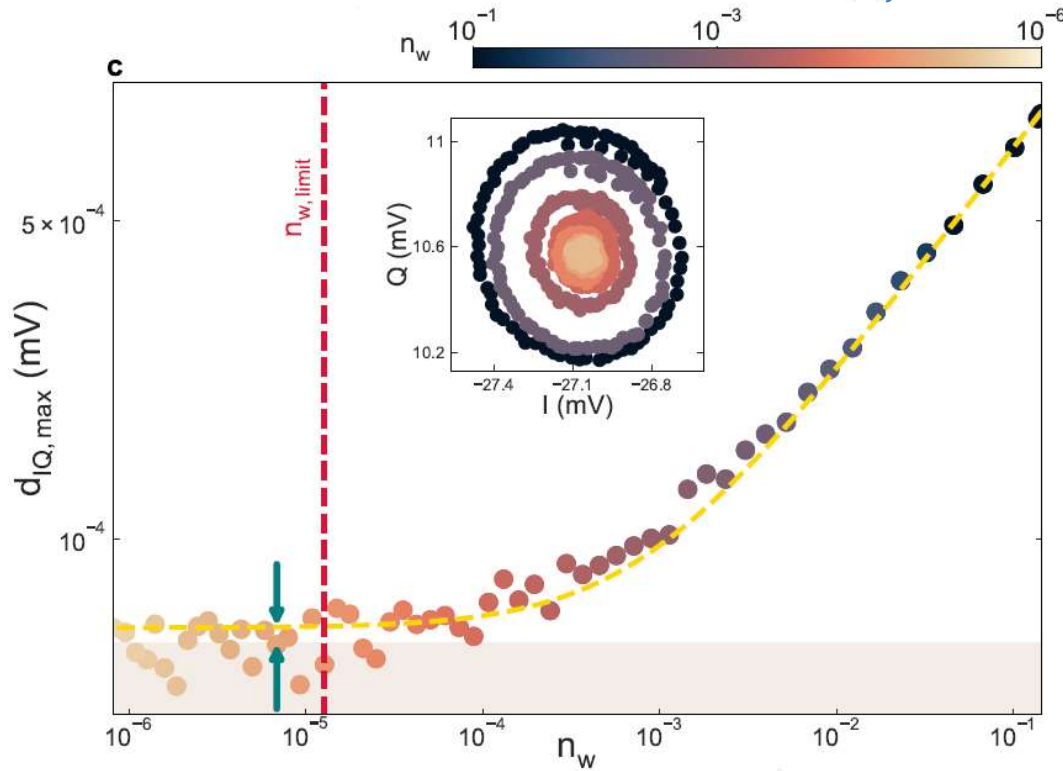
➔ Ramsey fringes are strongly modulated by interfering signal



➔ Detection at $\omega_{cav} = \omega_{fax}$

Quantum Enhancement Detection Method

Phase-resolved detection at $\omega_{cav} = \omega_{fax}$



C. Fruy, A. Théry, et al. (2026), *Phys. Rev. A* 113, 023706

n_ω = average photon number in the transmon drive pulse
 d_{IQ} = max distance between two points with the same amplitude

Increased sensitivity at cosmological limit

$$10^{-5} \text{ photons in 400 ms} \\ \equiv \\ 1.2 \times 10^{-2} \text{ } W/\sqrt{Hz}$$

Increased Figure of Merit (FoM)

$$F_{halo} = \frac{(\Omega_{ax}^0)^4}{\Lambda_a^3} \approx \text{mHz} \\ \ll \\ F_{phase} \approx \frac{\Omega_{ax}^2}{\Lambda_a^3} \approx 0.4 \text{ MHz}$$

A. Cottet and T. Kontos: *New J Phys* 28 024504 (2026)

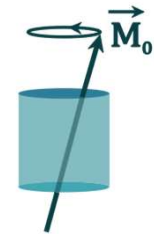
Research Project Goals

Key goals of AXION sensing:

➤ Expand the **mass scanning range**



Magnetic materials in resonant cavities



➤ Boost the **detection sensitivity**



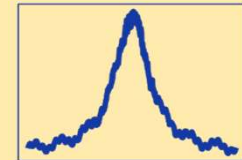
Non-linear coupling



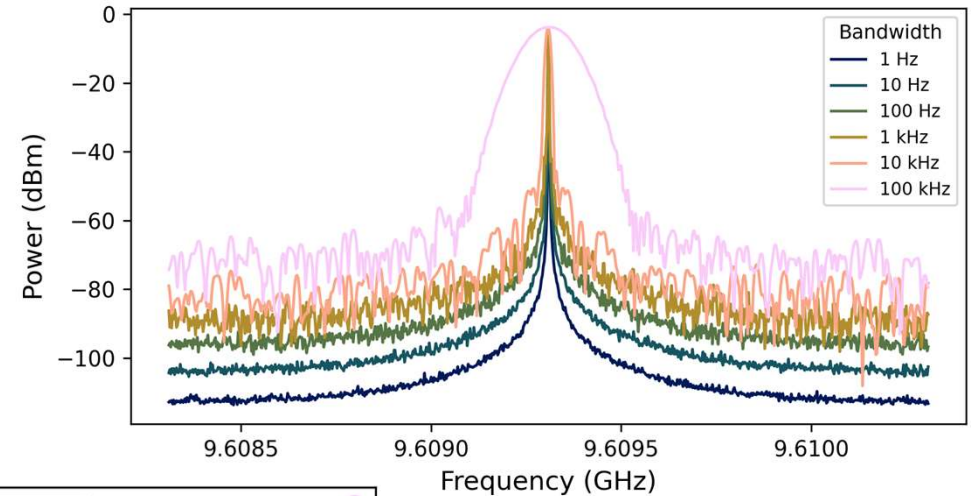
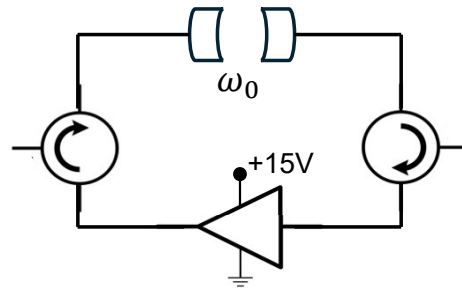
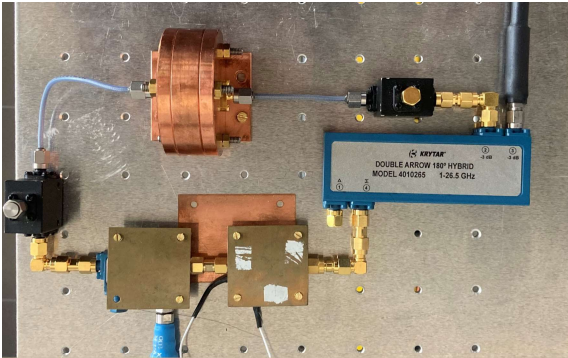
➤ Simulate a **fake axion** signal



Phase-jammed signal



Phase Jamming

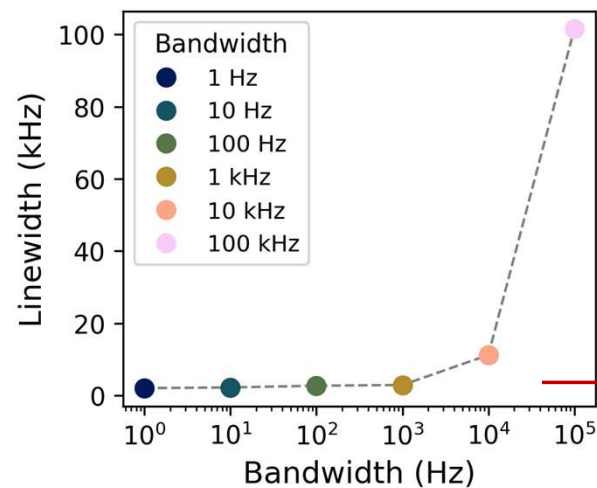


Power spectral density:

$$S(\theta) = \frac{kTF}{P_0} \left(1 + \frac{K\omega_\alpha}{\Delta\omega} \right)$$

- $\theta(t)$: random phase fluctuation
- F : noise figure
- P_0 : oscillator output power at ω_0
- $\Delta\omega$: frequency offset relative to ω_0
- K : flicker noise sensitivity (scaling factor)
- ω_α : corner angular frequency between flicker and white phase noise

David M. Pozar, *Microwave Engineering, 4th Edition, Wiley, 2012*



Measurement instrument- limited

true 1kHz source

more realistic fictitious axion source

Key Points and Outlooks

- **Large tunability** of the phase-resolved haloscope through gyromagnetic materials
- Technical focus on **mode (0, 1, 0) isolation** and manipulation
- Tri – partite coupling by implementing gyromagnetic modes in Chloe's detection setup
- Phase – jammed source to **simulate $\sim kHz$ linewidth axions**
- **Phase-jamming tunability** by using phase shifters in the MASER – like setup

Thank you for your attention !

Benchmarking Parameters

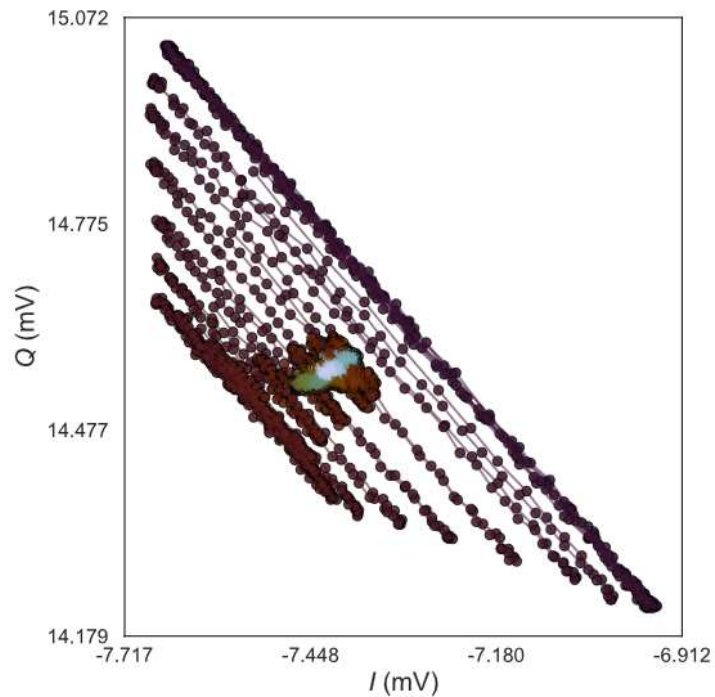
$\epsilon = 12\epsilon_0$	$\gamma = 2\pi \times 28 \text{ GHz}\cdot\text{T}^{-1}$	$\mu_0 M_0 = \mu_0 \rho g \mu_B S = 0.25 \text{ T}$
$\rho = 4.22 \times 10^{27} \text{ m}^{-3}$	$S = 5/2$	$a = 2.5 \text{ mm}$

Characteristic RADES measurement time	$1/T_{\text{RADES}} = 10^{-5} \text{ Hz}$
Magnetic flux density due to static magnetization	$\mu_0 M_0 = 0.25 \text{ T}$
Cavity volume	$V = 200 \cdot 10^{-3} \cdot \pi \cdot (2.5 \cdot 10^{-3})^2 \approx 3.9 \times 10^{-6} \text{ m}^3$
YIG permittivity	$\epsilon = 12\epsilon_0$
Gyromagnetic ratio	$\gamma = 2\pi \times 28 \times 10^9 \text{ Hz/T}$
Axion energy density	$\rho_{ax} = 0.45 \times 10^{15} \text{ eV/m}^3$

Quantum Enhancement Detection Method

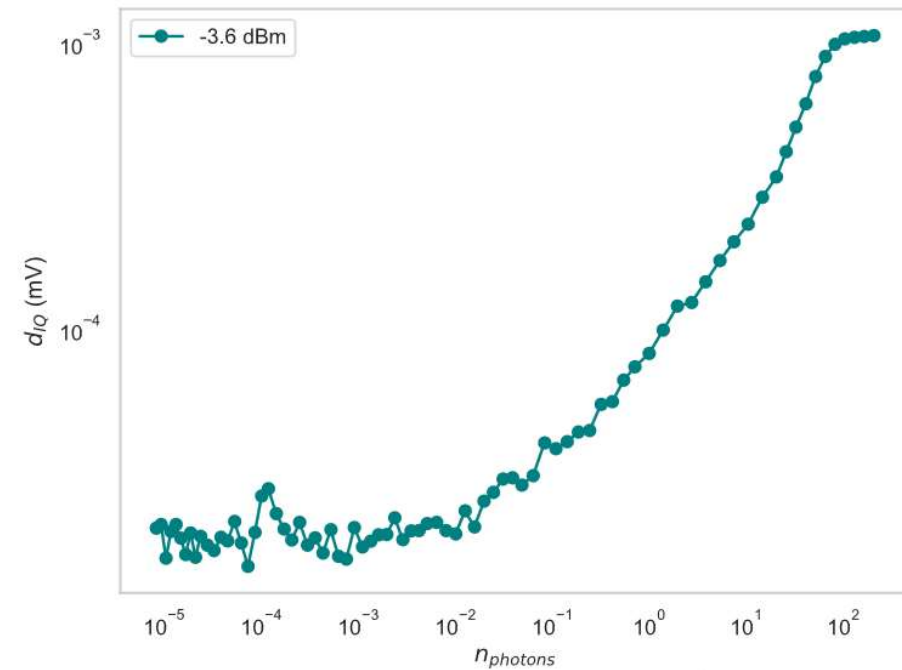
Phase-resolved detection at

$$\omega_{cav} = \omega_m = \omega_{fax}$$



C. Fruy, A. Théry, et al. (2026), Phys. Rev. A 113, 023706

Increased sensitivity



Sensitivity of 10^{-3} photons in 400 ms

➔ Need to increase the magnetic volume to improve sensitivity

Gyromagnetic Modes in Cylindrical Cavity

Solving the Maxwell equations in a cylindrical cavity with YIG tensor leads to the Helmholtz equation:

$$\frac{\partial^2 e_z}{\partial r^2} + \frac{1}{r} \frac{\partial e_z}{\partial r} + \frac{1}{r^2} \frac{\partial^2 e_z}{\partial \theta^2} + k^2 e_z = 0$$

with $k = \omega \sqrt{\mu_{\perp} \epsilon}$ and

$$\mu_{\perp} = \mu_0 \frac{\mu_r^2 - \mu_a^2}{\mu_r} = \mu_0 \frac{\gamma^2 \mu_0^2 (H_0 + M_0)^2 + 2i\eta\gamma\mu_0 (H_0 + M_0)\omega - (1 + \eta^2)\omega^2}{\gamma^2 \mu_0^2 H_0 (H_0 + M_0) + i\eta\gamma\mu_0 (2H_0 + M_0)\omega - (1 + \eta^2)\omega^2}$$

Spatial solution and boundary conditions:

$$e_z^{n,m,p}(r, \theta, z) = \sum_n \sum_m \sum_p (A_{nmp} \cos(n\theta) + B_{nmp} \sin(n\theta)) \sin(k_{\parallel p} z) J_n(k_{\perp nm} r)$$

$$\text{with } k_{n,m,p} = \sqrt{k_{\perp nm}^2 + k_{\parallel p}^2} \quad \text{with } \begin{cases} k_{\perp nm} = \frac{z_{nm}}{a}, & \text{where } z_{nm} \text{ is the } m^{\text{th}} \text{ root of } J_n \\ k_{\parallel p} = \frac{p\pi}{L}, & \text{where } p \text{ is an integer} \end{cases}$$

Consider $\eta = 0$, the magnetic dissipation, then:

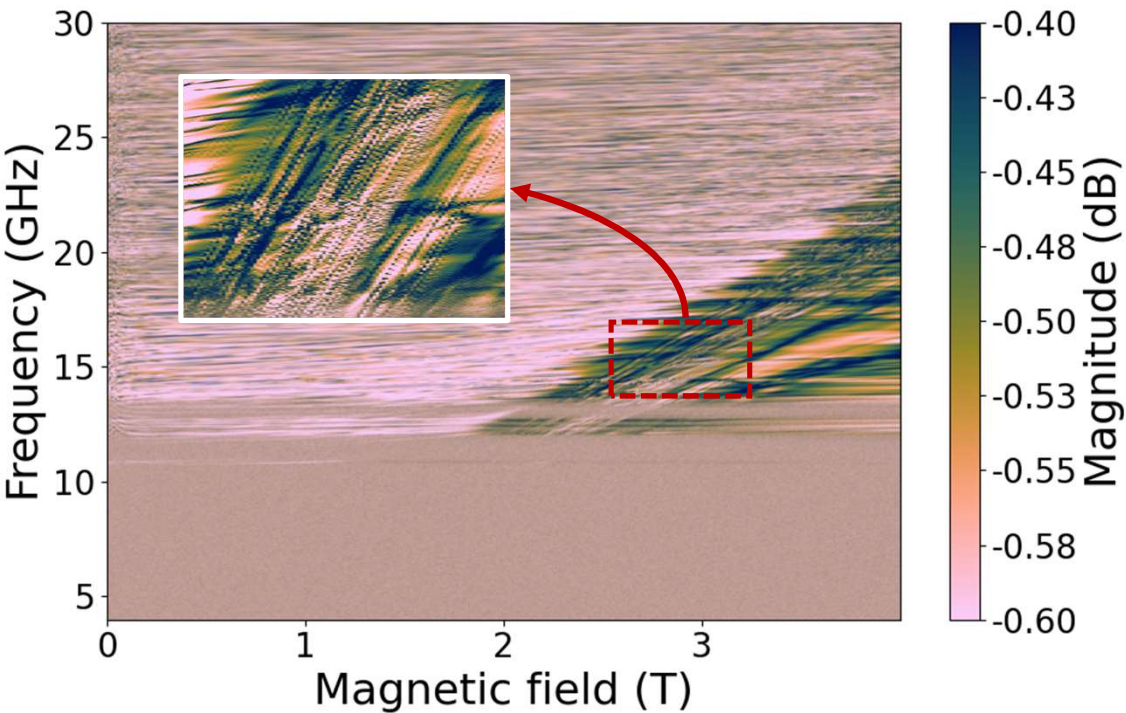
$$\omega_{nmps} = \frac{\sqrt{\mu_0^2 \gamma^2 (H_0 + M_0)^2 + \Omega_{nmp}^2 + s \sqrt{\mu_0^4 \gamma^4 (H_0 + M_0)^4 - 2\mu_0^2 \gamma^2 (H_0^2 - M_0^2) \Omega_{nmp}^2 + \Omega_{nmp}^4}}}{\sqrt{2}}$$

with

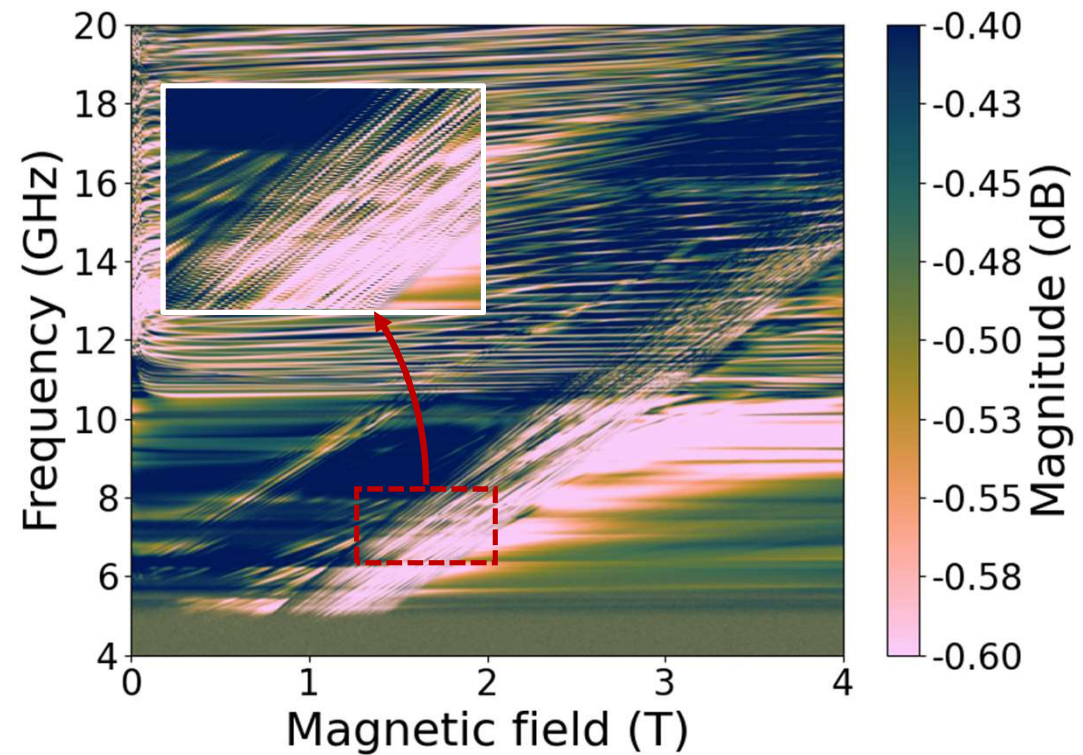
$$s = \pm 1 \quad \text{and} \quad \Omega_{nmp}^2 = \frac{1}{\epsilon \mu_0} \left(\left(\frac{z_{nm}}{a} \right)^2 + \left(\frac{p\pi}{L} \right)^2 \right)$$

Gyromagnetic Modes Measurements

Copper barillet and teflon holders



Copper barillet and direct coaxial excitation



Coupling Strength

The coupling Hamiltonian:
$$H_c = \frac{1}{\mu_0 c} g_{a\gamma\gamma} \cos(\omega_{ax}t - \varphi_{ax}) \iiint r dr d\theta dz \vec{E} \cdot \vec{B}$$

Time harmonic solution to the Helmholtz equation:

$$\vec{E} = \vec{e}(r, \theta, t) = - \sum_{n,m} i\omega_{nm} J_n(k_{nm}r) (\sin(n\theta) + B_{nm} \cos(n\theta)) (A_{nm} e^{i\omega_{nm}t} - A_{nm}^* e^{-i\omega_{nm}t}) \hat{z}$$

 Magnetic field:

$$\vec{B} = \mu_0(M_0 + H_0)\hat{z} + \vec{b}(r, \theta, t)$$

$$H_c = \sum_m \hbar \cos(\omega_{ax}t - \varphi_{ax}) \Omega_{ax}^m (\hat{m}_{0m} + \hat{m}_{0m}^\dagger)$$

with the coupling strength
$$\Omega_{ax}^m = \frac{1}{\hbar \mu_0 c} g_{a\gamma\gamma} \mu_0 (M_0 + H_0) \frac{1}{z_{0m}} \sqrt{\frac{2V}{\epsilon}} \hbar \omega_{0m}$$

Form Factor

$$C = \frac{\langle \mathbf{E} \cdot \mathbf{B}_0 \rangle_{|\psi\rangle}^2}{\langle \mathbf{B}_0 \cdot \mathbf{B}_0^* \rangle_{|\psi\rangle} \langle \mathbf{E} \cdot \mathbf{E}^* \rangle_{|\psi\rangle}}$$

$$\bullet \quad \langle \mathbf{E} \cdot \mathbf{B}_0 \rangle^2 = \mu_0^2 (M_0 + H_0)^2 \hbar \frac{2}{V_a \epsilon} \left\langle \sum_m \frac{1}{z_{0m}} \sqrt{\omega_{0m}} (\hat{m}_{0m}^\dagger + \hat{m}_{0m}) \right\rangle_{|\psi\rangle}^2 \longrightarrow \langle \mathbf{E} \cdot \mathbf{B}_0 \rangle_{|0\rangle}^2 = \mu_0^2 (M_0 + H_0)^2 \hbar \frac{2}{V_a \epsilon} \sum_m \frac{\omega_{0m}}{z_{0m}^2}$$

$$\underbrace{\qquad\qquad\qquad}_{[\hat{m}_{0m}^\dagger, \hat{m}_{0m'}] = \delta_{mm'}}$$

$$\bullet \quad \langle \mathbf{B}_0 \cdot \mathbf{B}_0^* \rangle_{|0\rangle} = \mu_0^2 (H_0 + M_0)^2$$

$$\bullet \quad \langle \mathbf{E} \cdot \mathbf{E}^* \rangle_{|0\rangle} = \hbar \frac{1}{2V_a \epsilon} \sum_m \omega_{0m}$$

For one mode (n, m, s) $C^m = \frac{4}{z_{0m}^2}$ with $z_{0m} = \pi \left(m - \frac{1}{4} \right) + \mathcal{O}(m^{-1})$ the m^{th} root of J_0

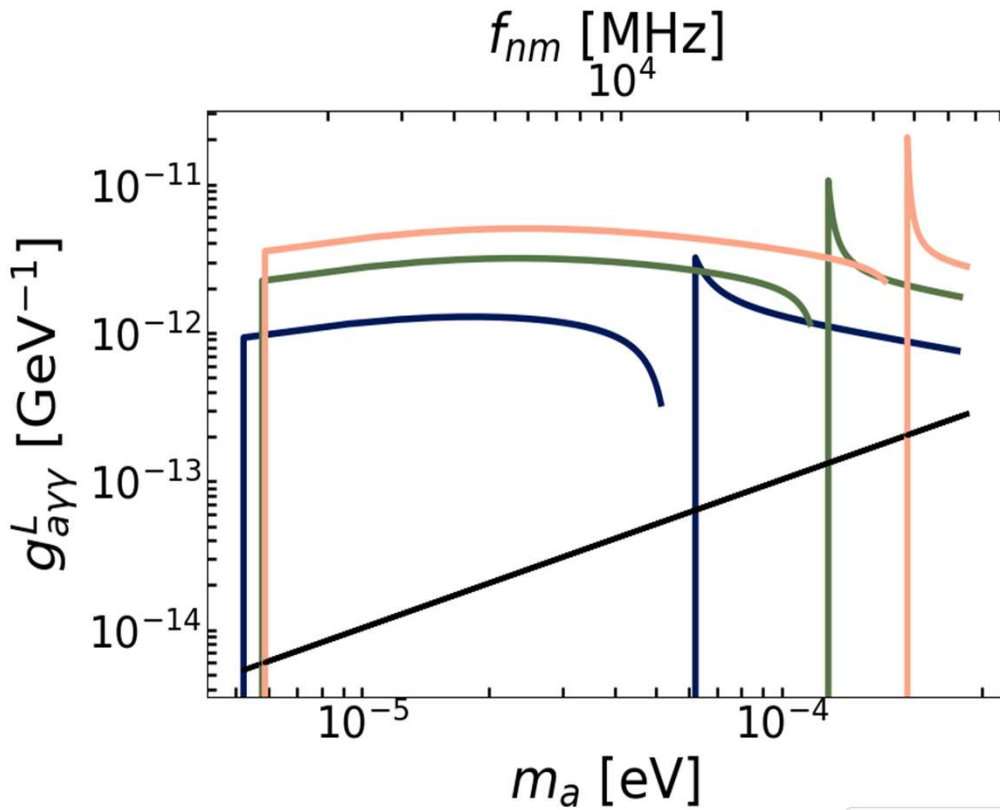
Conventional Haloscope SNR

$$SNR = \frac{\Delta P_0}{\sqrt{\nu_0}} \quad \text{A. Cottet, kT. Kontos 25'}$$

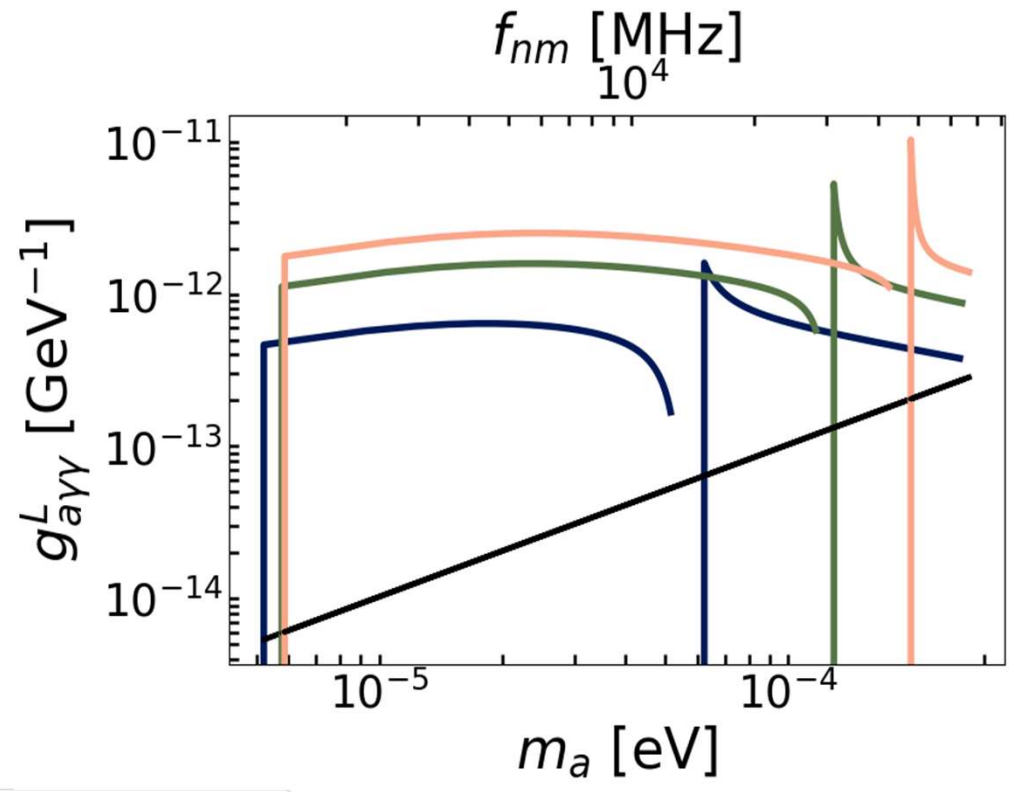
- $\Delta P_0 = \frac{2(\Omega_{ax}^0)^2}{\Lambda_a^2}$ amplitude of the axionic signal at resonance
 - $\nu_0 = \frac{4(1+2n_B)}{\Lambda_a T}$ signal variance
- $SNR = 1 \leftrightarrow \frac{\Omega_{ax}^4}{\Lambda_a^3} = \frac{1}{T} = F_{halo}$

First 3 Modes Coupling Constant

1 cavity



4 cavities in parallel



Phase-Jammed Source Setup

Amplifier

<https://nardamiteq.com/docs/MITEQ-AFS.PDF>

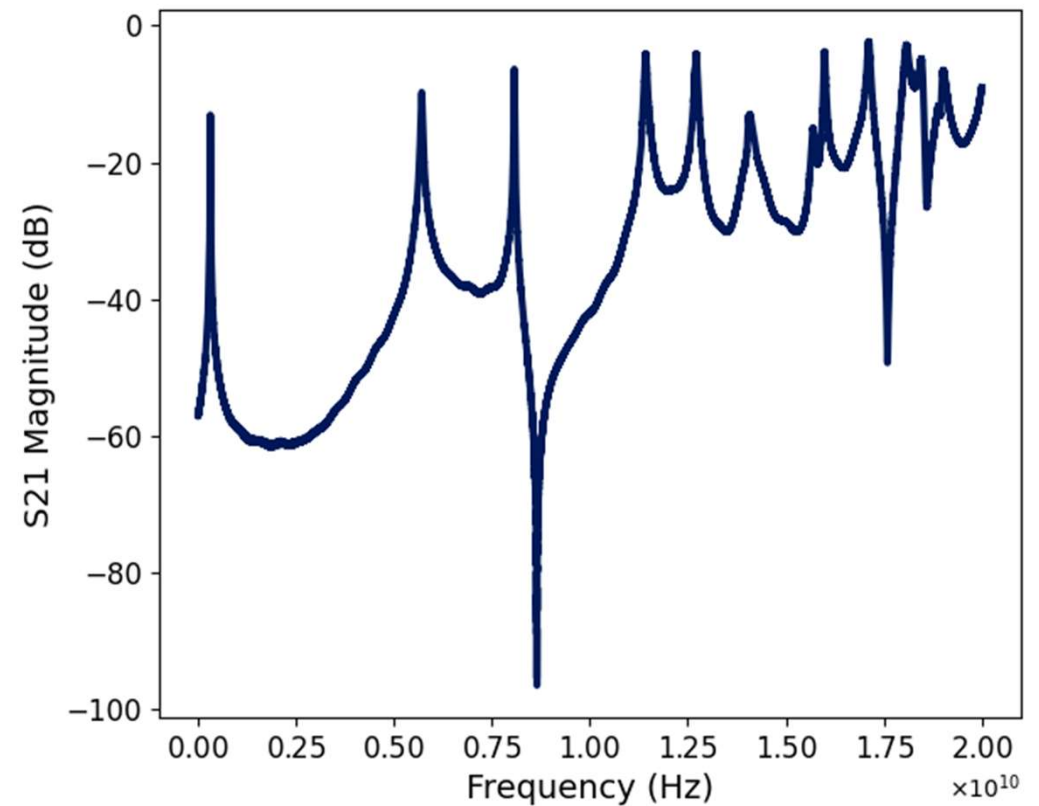
Model : AFS3-04000800-07-10P-4

Freq. range (GHz) : 4 – 8

Gain (dB) : 28

Noise Figure : 0.7

Cavity resonator spectrum



Ramsey Experiment: Bloch Sphere

